Journal of Science and Technology ***54*** *(4) (2016) 545-556*

DOI: 10.15625/0866-708X/54/4/6231

DESIGN ANALYSIS FOR A SPECIAL SERIAL - PARALLEL MANIPULATOR

Chu Anh My[1, *], Vuong Tien Trung[2]

[1]*17 Mechanical Company, Dong Xuan, Soc Son, Hanoi*

[2]*Advanced Technology Center, Le Quy Don Technical University, 236 Hoang Quoc Viet, Hanoi*

[*]Email: *mychuanh@yahoo.com*

Received: 21 May 2015; Accepted for publication: 9 May 2016

ABSTRACT

This paper presents a design of serial - parallel manipulator for transferring heavy billets for a hot extrusion forging process. To increase the structural rigidity and restrict the end-effector of the robot moving in direction parallel with the ground surface, parallel links were added in between serial links of the manipulator. To validate the design, the kinematic modeling, the kinematic performance analysis and the strength analysis for the robot were taken into account. With respect to the parallel links, the constraint equation was written and put together with the kinematic model. Based on the model formulated, the inverse kinematic, the transferring time, the reachable workspace, the dexterity, and the manipulability index of the robot were analyzed and discussed to demonstrate its kinematical performance. These results are important to assess the working capability and improve the parametric design for the robot. In addition, for verifying the end-effector design in terms of the strength and displacement, the stress distribution and the static deflection of the end-effector module were computed and analyzed by using the computer-aided finite element method (FEM).

Keywords: robotics, mechatronics system, industrial robot design.

1. INTRODUCTION

Forging is a manufacturing process involving the shaping of metal using localized compressive forces. In general, a hot forging station usually composes of a heating furnace and a forging machine that uses either a hydraulic press or mechanical press for the billet extrusion. Consider a specific hot forging station described in Fig. 1. At the beginning of a processing cycle, workers grip a billet, weighted about 60 kg, from the billet loading area (Position 1), move and place it onto the heating furnace (Position 2). When the temperature of the billet in the furnace reaches to 1100^0C, the workers grip the billet again and transfer it into the die mounted on the forging machine (Position 3). After that the forging operation stars to extrude the billet as required.

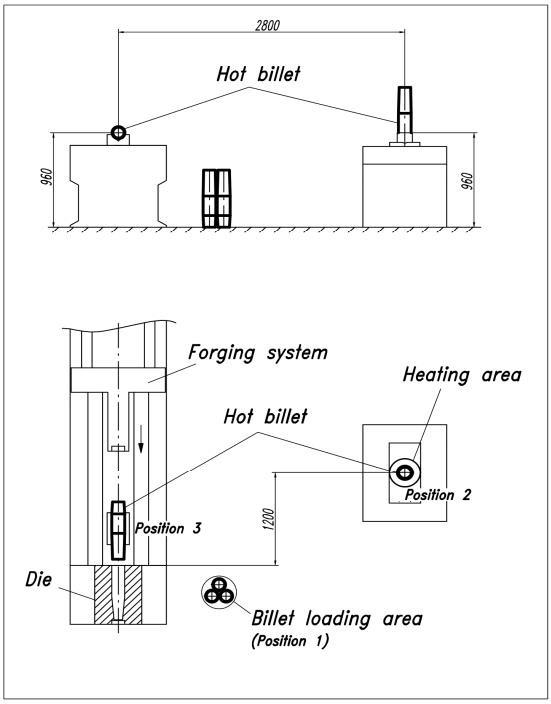

Figure 1. Layout of the extrusion forging station.

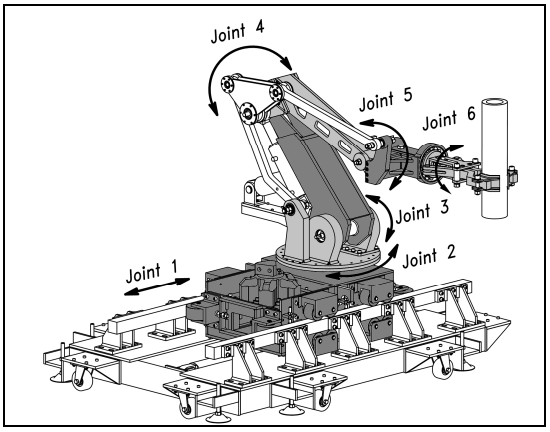

Figure 2. CAD model of the manipulator.

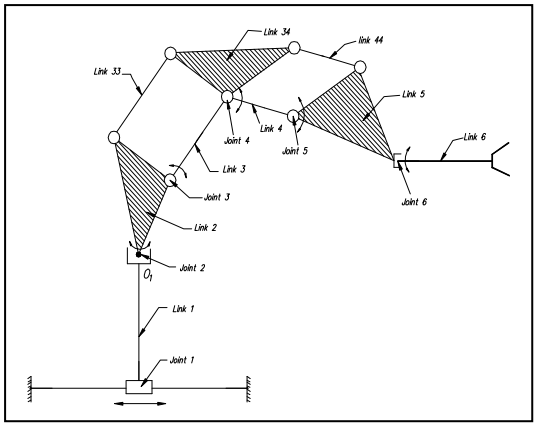

Figure 3. The schematic diagram of the manipulator.

This manual transferring method increases the downtime and consumes the energy and manpower. Therefore, an industrial manipulator is needed for supporting the workers handling the billet. Figure. 2 shows the 3D manipulator design, and Fig. 3 presents the schematic diagram of the robot. The design consists of a fixed base and 9 links jointed by kinematical joints with one degree of mobility. The prismatic joint 1, rotary joints 3 and 4 are driven by hydraulic actuators, respectively. Link 33, link 34 and link 44 are added to close two local kinematics chains. These additions are to increase the loading capacity of the structure and restrict the

orientation of the end-effector (link 6). In all cases, the end-effector moves in parallel with the horizontal ground surface. The restriction of the end-effector's orientation makes it convenient when the robot picks up a billet and releases it onto the heating table. In other words, this advantage could help to reduce the complexity of the controlling procedure. Though the proposed design of the hybrid serial-parallel links shows its advantages mentioned, it possesses complexity in modeling and controlling.

For designing and controlling the robot, the kinematics modeling and kinematics performance analysis play a central role that need to be considered specifically. In particular, the static deflection of the end-effector, the stress and the displacement distribution on the the end-effector should be taken into account since the manipulator suffers a heavy payload. The kinematic of general serial manipulators has been the fundamental problem. Further studies in this area could be found in the literature such as the kinematics design of manipulator [1], the kinematic of the redundant robot [2], the kinematic of the parallel robot [3, 4]. Modeling and analyzing the design of serial manipulators suffering heavy payload, there has been a number of researches [5 - 8]. However, a few researchers interests in modeling and analyzing the hybrid serial - parallel robot structures. In the area of studying on the elastic deformation of the robot structure, the related researches mostly focus on the mathematical modeling of displacement and control of flexible robot [9, 10]. The paper [9] proposes a systematic approach to assess the accuracy of a parallel kinematic machine subject to structural errors and then to effectively compensate for them. Analytical models were constructed for both the nominal and actual structures. The literature review on the state-of-the-art for flexible manipulators [10] reveals that the dynamic analysis and control of flexible manipulators is an emerging area of research in the field of manufacturing, automation, and robotics due to a wide spectrum of applications starting from simple pick and place operations of an industrial robot to micro-surgery, maintenance of nuclear plants, and space robotics. Using the computer-aided finite element approach, researches presented in [11, 12] consider the analysis of how the stress and displacement distributed on links designed with given geometry and material. However, the analysis models in [11, 12] need more detailed calculation of applied torques and forces for links which require the strength analysis specifically. Putting the entire design model of the complex manipulator into finite element calculation and simulation would cause complexity in analyzing alternatives.

This paper presents a validation for the design of the robot. The numerical method is employed to analyze the forward and inverse kinematic behavior of the system. Kinematic performance of the design is investigated and discussed also. Finally, the maximum static deflection and the stress distribution on the end-effector are computed by using the computer-aided finite element approach (FEM). The presented methodology could be economical and useful for checking up the strength and the loading capacity of the same manipulators designated to handle heavy billets.

2. KINEMATICS MODELING

In Figure 4 we denote $\mathbf{q} = \begin{bmatrix} d_1 & q_2 & q_3 & q_4 & q_5 & q_6 \end{bmatrix}^T$ as the vector of joint variables. $O_0 \equiv (O_0 x_0 y_0 z_0)$ is the reference frame; $O_1, O_2, ...,$ and O_6 are the link frames, correspondingly. The coordinate systems 1' and 5' are added to write all the homogeneous transformation matrixes of the whole system in the same formulation by Denavit-Hartenberg, $\mathbf{H}_{ji}(\theta_i, d_i, a_i, \alpha_i)$. The matrix $\mathbf{H}_{ji}$ characterizes the homogeneous motion of the frame

indexed i with respect to the preceded frame indexed j, where θ_i, d_i, a_i and α_i are the kinematical and geometrical parameters refer to the index i; for the kinematical model , all the parameters are listed in Tab. 1.

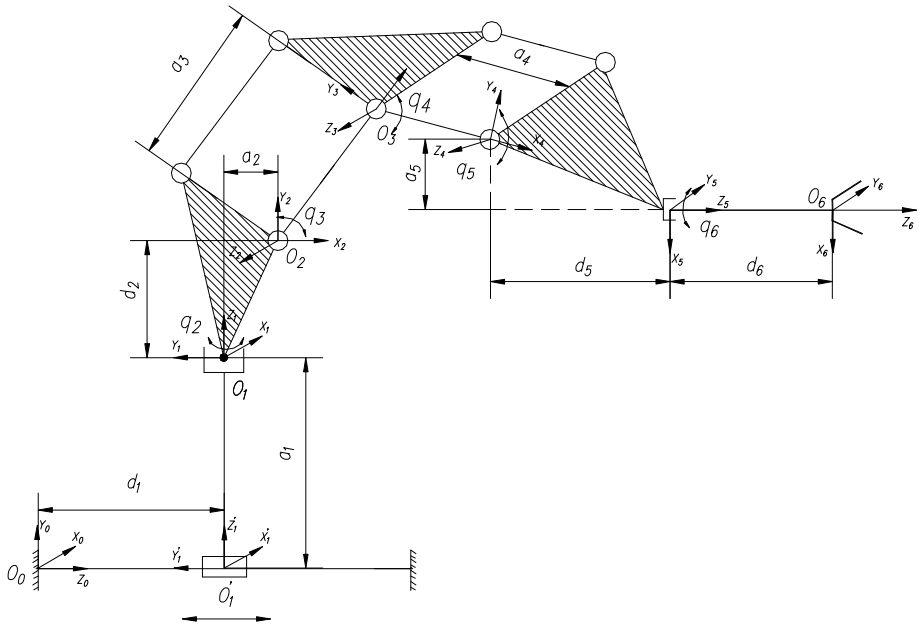

Figure 4. Kinematical model.

Table 1. Kinematical and geometrical parameters.

i	θ_i	d_i	a_i	α_i
1’	0	d_1	0	$-\pi/2$
1	0	a_1	0	0
2	q_2	d_2	a_2	$\pi/2$
3	q_3	0	a_3	0
4	q_4	0	a_4	0
5’	q_5	0	a_5	$-\pi/2$
5	0	d_5	0	0
6	q_6	d_6	0	0

In the reference frame, the homogeneous transformation matrix of the end-effector can be written as

$$\mathbf{H}_{0E} = \begin{bmatrix} \mathbf{A}_{0E} & \mathbf{r}_E \\ 0 & 1 \end{bmatrix}, \tag{1}$$

where $\mathbf{r}_E = \begin{bmatrix} x_E & y_E & z_E \end{bmatrix}^T$ represents the position (the reference point) and $\mathbf{A}_{0E}$ is the rotation matrix of the end-effector.

Multiplying all the transformation matrixes yields

$$\mathbf{H}_{0E} = \mathbf{H}_{01'}(d_1)\mathbf{H}_{1'1}\mathbf{H}_{12}(q_2)\mathbf{H}_{23}(q_3)\mathbf{H}_{34}(q_4)\mathbf{H}_{45'}(q_5)\mathbf{H}_{5'5}\mathbf{H}_{56}(q_6) \quad (2)$$

Substituting the parameters in Tab. 1 into Eq.(2) yields

$$\mathbf{H}_{0E} = \begin{bmatrix} \mathbf{A}_{06}(\mathbf{q}) & \mathbf{r}_{06}(\mathbf{q}) \\ 0 & 1 \end{bmatrix}.$$

Therefore,

$$\begin{bmatrix} \mathbf{A}_{0E} & \mathbf{r}_E \\ 0 & 1 \end{bmatrix} = \begin{bmatrix} \mathbf{A}_{06}(\mathbf{q}) & \mathbf{r}_{06}(\mathbf{q}) \\ 0 & 1 \end{bmatrix} \quad (3)$$

Equation (3) describes the forward kinematic relationship of the robot.

If we denote $\mathbf{p}_E = [x_E \quad y_E \quad z_E \quad \gamma \quad \beta]^T$ representing the general position of the end-effector in O_0, where γ is the yaw angle and β is roll angle of the end-effector, Eq. (3) can be rewritten as

$$\mathbf{p}_E = \mathbf{f}(\mathbf{q}) \ . \quad (4)$$

Due to the motion feature of the two parallel links, for every configuration of the system, the relative position of the frames O_2, O_3 and O_4 is shown in Fig. 5. Based on this special topology relationship, the constraint equation for the system motion can be written as

$$q_5 = -q_3 - q_4 - \frac{\pi}{2}. \quad (5)$$

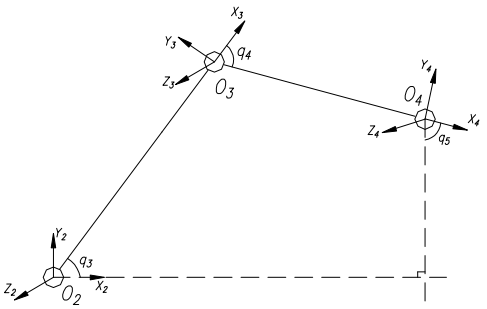

Figure 5. The relationship among q_3, q_4 and q_5.

Eqution (5) shows that the joint variable q_5 is dependent. Therefore, the Eq. (4) has only 5 independent variables. Physically, the joint 5 is passive; there is no actuator needed for deriving the joint. Substituting Eq. (1) into (5), and solving for $\mathbf{p}_E$ yields

$$\mathbf{p}_E = \begin{bmatrix} \cos q_2[a_4\cos(q_3+q_4)+a_3\cos q_3+a_2+d_5+d_6] \\ a_4\sin(q_3+q_4)+a_3\sin q_3+a_1-a_5+d_2 \\ -\sin q_2[a_4\cos(q_3+q_4)+a_3\cos q_3+a_2+d_5+d_6]+d_1 \\ q_2 \\ q_6 \end{bmatrix} \tag{6}$$

3. INVERSE KINEMATIC AND KINEMATIC PERFORMANCE DISCUSSION

3.1. Inverse Kinematic Analysis

To keep the temperature of the heated billet during the transferring, the robot must move fast enough so that the transferring time is not greater than 22s. In order to analyze the time transferring, and determine the joint variables according to the given task, the inverse kinmatic model needs to be analyzed.

Based on Eq. (6), the inverse kinematic problem is formulated as

$$\mathbf{q} = \mathbf{f}^{-1}(\mathbf{p}_E). \tag{7}$$

Given $\mathbf{p}_E$, solving Eq.(7) yields the analytical solution of the inverse kinematic as follows.

$$q_6 = \beta, \tag{8}$$

$$q_2 = \gamma. \tag{9}$$

$$d_1 = x_E\tan q_2 + z_E, \tag{10}$$

$$q_4 = \cos^{-1}\left(\frac{\left(\frac{x_E}{\cos q_2}-A\right)^2+(y_E-B)^2-a_3^2-a_4^2}{2a_3a_4}\right), \tag{11}$$

$$q_3 = \tan^{-1}\left(\frac{-b+\sqrt{b^2-4ac}}{2a}\right), \tag{12}$$

where $A = a_2+d_5+d_6$; $B = a_1-a_5+d_2$; $a = -(y_E-B)^2+(a_4\cos q_4+a_3)^2$;
$b = 2a_4\sin q_4(a_4\cos q_4+a_3)$; $c = -(y_E-B)^2+a_4^2\sin^2 q_4$.

Equations (8)-(12) show that for any point $\mathbf{p}_E = [x_E \quad y_E \quad z_E \quad \gamma \quad \beta]^T$ given in the workspace, we can determine the value of $\mathbf{q}$ analytically. It is noticeable that the inverse computation found is independent of time. For real time control programming, the time-varying history of joint variables $\mathbf{q}(t)$ must be determined according to the required end-effector trajectory, $\mathbf{p}_E(t)$, represented in time domain. Therefore, the desired path $\mathbf{p}_E(t)$ should be planned. The planning procedure can be summarized as follows.

Based on the control points $\mathbf{P}_0$, $\mathbf{P}_1$, $\mathbf{P}_2$,..., and $\mathbf{P}_n$ chosen in the workspace, a parametric curve, $\mathbf{p}_E(u)$, representing the end-effector path is formulated, where $u \in [0,1]$. Calculating the arc length of $\mathbf{p}_E(u)$ yields $s(u) = \int_0^u \sqrt{\left(\frac{dx_E}{du}\right)^2 + \left(\frac{dy_E}{du}\right)^2 + \left(\frac{dz_E}{du}\right)^2}\, du$. Based on the required velocity profile $\dot{s}(t)$ of the end-effector along the path, the arc length $s(t)$ is also calculated as $s(t) = \int_0^t \dot{s}(t)dt$. Based on $s(t)$ and $s(u)$ numerically computed, the time-varying parameter $u(t)$ is determined by some numerical interpolation such as the function *spline* available in Matlab: $u(t_i) = spline\left[s(t_i), t_i, s(u_i)\right]$. Substituting $\{u(t_i)\}$ into $\mathbf{p}_E(u)$ yields $\mathbf{p}_E(t)$.

Consider the designing robot. The geometric parameters of the links are given as a_1 = 0.11 m, d_2 = 0.25 m, a_2 = 0.1 m, a_3 = 0.73 m, a_4 = 0.63 m, a_5 = 0.81 m; d_5 = 0.03 m and d_6 = 0, 43 m. Suppose that $\dot{s}(t) = 0.15\, m/\text{sec}$ is the velocity of the end-effector in the steady motion state. The parametric curve representing the required path, $\mathbf{p}_E(u)$, is planned on the selected control points as

$$\mathbf{P}_0 = [1.7062 \quad 0.6962 \quad 0.5 \quad 0.0 \quad 0.0]^T,\ \mathbf{P}_1 = [1.114 \quad 0.8435 \quad 0.5 \quad 0.0 \quad 0.0]^T,$$

$$\mathbf{P}_2 = [0.7844 \quad 0.8422 \quad 0.5 \quad 0.0 \quad 0.0]^T,$$

and

$$\mathbf{P}_3 = \left[0.1054 \quad 0.8883 \quad 1.8501 \quad \pi/2 \quad -\pi/2\right]^T.$$

By using the presented procedure, the required curve

$$\mathbf{p}_E(t) = \left[x_E(t) \quad y_E(t) \quad z_E(t) \quad \gamma(t) \quad \beta(t)\right]^T$$

is obtained. Based on the input $\mathbf{p}_E(t)$, the output $d_1(t)$, $q_2(t)$, $q_3(t)$, $q_4(t)$, and $q_6(t)$ are calculated by implementing Eqs. (8) - (12). Figure 6 shows such the numerical solution to the inverse kinematic equation of the Robot.

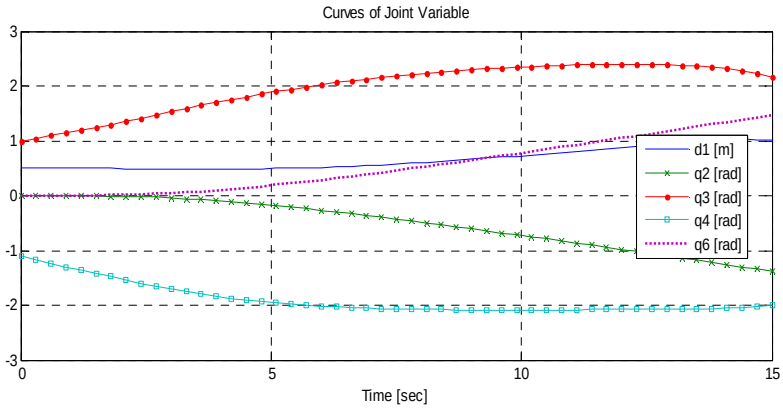

Figure 6. Time history of joint variables.

In the case of transferring billets for the forging process, none of the joint variables changes outside their feasible range. By using this analysis technique it is important to show that at the given velocity $\dot{s}(t) = 0.15 m/\sec$, the transferring time period is 15s.

3.2. Reachable Workspace Analysis

Based on the forward kinematic equation, the boundary of the reachable workspace is determined with respect to the specification of the kinematic configuration and the feasible range of joint variables such as $d_{1\max} \geq d_1 \geq d_{1\min}$, $2k\pi \geq q_2, q_6 \geq -2k\pi$ and $q_{3a} \geq q_3 \geq q_{3b}$. The following Fig. 7 shows the workspace volume in the case that $d_{1\max} = 1m$, $d_{1\min} = 0$, $q_{3a} = \pi/2$, $q_{3b} = 0$ and $q_4 = 0$. Notice that the end-effector always locates inside the space found for all cases that $0 > q_4 > -\pi$ and $\pi \geq q_3 \geq \pi/2$.

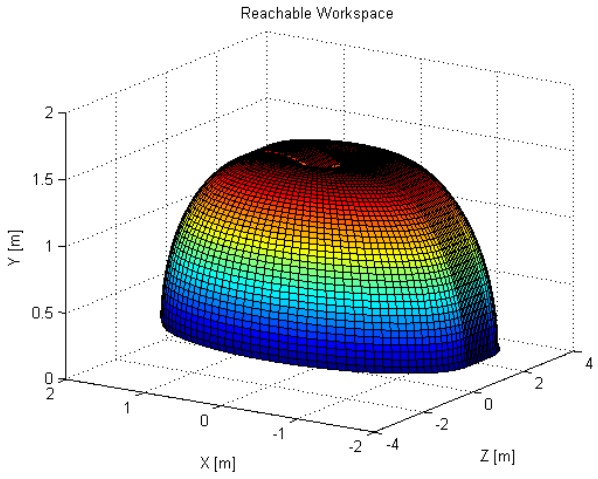

Figure 7. Reachable workspace.

It can be observed that the designing Robot can travel all the positions required (Position 1, Position 2 and Position 3) to sever the forging process, even it can be used for other extended applications.

3.3. Dexterity Analysis

The kinematic manipulability index, $\omega = \sqrt{\det(\mathbf{J}\mathbf{J}^T)}$, where $\mathbf{J}(\mathbf{q}) = \frac{\partial \mathbf{P}_E}{\partial \mathbf{q}} \in R^{5\times 5}$ is the Jacobian matrix, plays an essential role in the kinematical performance analysis since it indicate of how close the manipulator configuration is to the singularity. It should be shown that in which region of $\mathbf{q}$, the index is large enough to avoid singularities, and within this region, the manipulator operates under the desirable dexterity condition. The index for the Robot design is calculated as

$$\omega = a_3 a_4 \left|\sin q_4 \cos q_2\right|. \tag{13}$$

Eq. 13 shows that the index depends on q_2 and q_4 only. The singularity of the Robot is independent of d_1, q_3, and q_6. As seen in Fig. 8, the Robot should operate so that the joint variables q_2 and q_4 change outside the regions around $q_2 = \pm\pi/2$, $q_4 = 0$ and $q_4 = -\pi$. $\omega \to \max$ if $q_2 = 0$ and $q_4 = -\pi/2$.

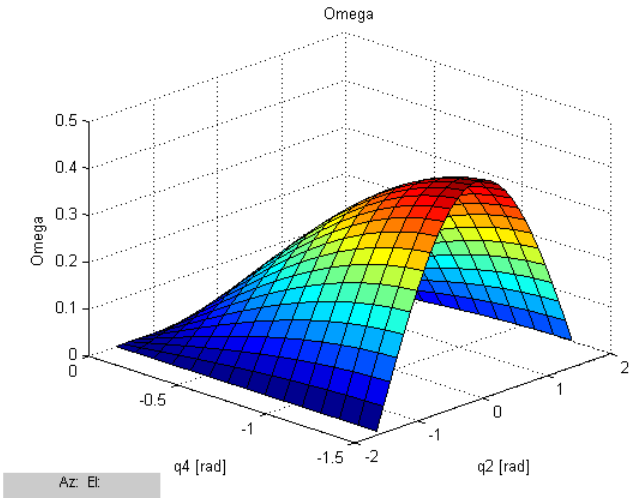

Figure 8. The manipulability index vs q_2 and q_4.

In addition, Eq. (13) shows that the manipulability index depends on the geometric parameters a_3 and a_4. The index varies along with the ratio $ka = a_4 / a_3$, in the case that $a_3 + a_4 = const$ and q_2 is given. The value of ka effects not only on the dexterity, but also on the structural parametric of the manipulator. If ka increases, the index ω will increase, but the stability margin of the system could decrease since the horizontal distance from the gravity center of link 4 to O'_1, the link's mass and inertia increase. In contrast, if a smaller ka is chosen, the lower limitation of the range of q_4 should be extended to maintain the dexterity of the Robot. For the designing Robot, the length of links 3 and 4 is chosen as $a_3 = 0.73m;\ a_4 = 0.63m$. The lower limitation of q_4 is checked with $q_{4\min} = -1.971rad$.

4. ANALYSIS OF STRESS AND DISPLACEMENT DISTRIBUTION ON THE END-EFFECTOR

Focusing on the structural deformation and strength, structural analysis is a key part of the engineering design of robot structure. For simple structures of manipulator, the stress and displacement fields distributed on components could be determined analytically to check up the strength of the designed parts. However, for complex structural manipulators, the use of robust computational techniques aided by computer reveals its efficiency and accuracy for the analysis. For the considering Robot, the end-effector's strength needs to be considered because the heavy payload is applied. In this section, the static stress and displacement distribution on the end-effector module are computed and simulated by using the finite element method integrated in

CAE software Autodesk Inventor (Ansys Machenical). Consequently, the maximum value of the stress and the deflection of the end-effector are determined to exam the safety factor and the loading capability of the Robot. Figure 9 presents the 3D model of the end-effector module acted by the external forces: $P_b = 589$ N (the billet gravity), $R_b = 981$ N (the force that the billet reacts to the griper), $P_e = 677$ N (the end-effector gravity), and R (the force that the ball bearing reacts to the structure).

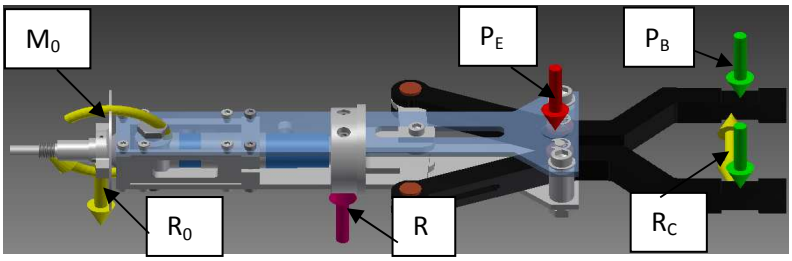

Figure 9. Structural analysis model for the end-effector module.

To determine the unknown force R, the following structural model in Fig. 10 is considered.

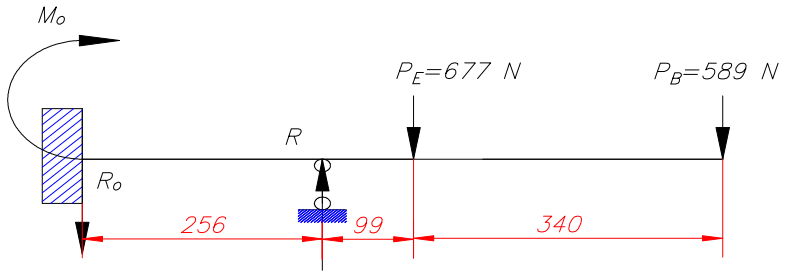

Figure 10. Simplified model to determine R.

Denote $y_1(z)$, $y_2(z)$ and $y_3(z)$ as the displacements along three segments R_0R (256 mm), RP_e (99 mm), and P_eP_b (340 mm). The constant EJ characterizes the elastic property of the material. Solving the following equations (14) - (18), in which Eqs. (16) - (18) represent the continuous vertical displacement of the end-effector yields $R_0 = 277\ N$, $R = 1563\ N$, and $M_0 = 23637\ N.mm$.

$$R = P_e + P_b + R_0 \tag{14}$$

$$(256+99)P + (256+99+340)P_b = 256R + M_0 \tag{15}$$

$$y_1(z) = -\left(\frac{1}{EJ}\right)\left(\frac{M_0 z^2}{2} - \frac{R_0 z^3}{6}\right),\ 0 \le z \le 256 \tag{16}$$

$$y_2(z) = y_1(z) - \left(\frac{1}{EJ}\right)\left[\frac{R(z-256)^3}{6}\right],\ 256 \le z \le 355 \tag{17}$$

$$y_3(z) = y_2(z) - \left(\frac{1}{EJ}\right)\left[\frac{-P_e(z-256-99)^3}{6}\right],\ 355 \le z \le 695 \tag{18}$$

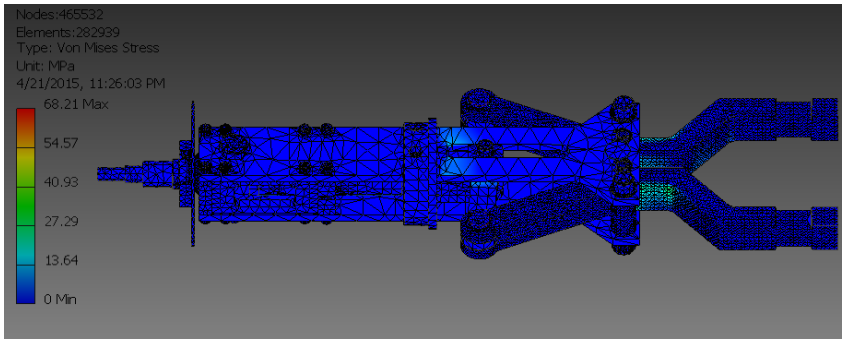

Figure 11. The stress distribution.

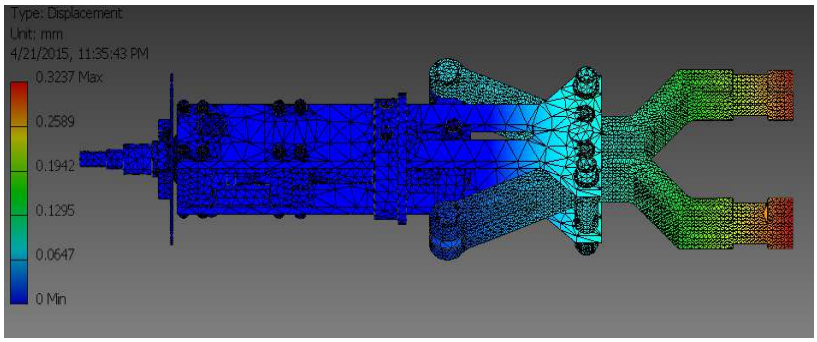

Figure 12. Displacement of the module.

Assigning all obtained values of moment and forces and running the analysis model on the software, the distribution of the stress, safety factor and displacement are yielded and they are shown in Figs. 11 and 12, respectively.

As depicted in Fig. 11, the maximum stress is 68.21 Mpa that is much lesser than the yield strength of the designated material, $[\sigma] = 99$ MPa . As seen in Fig. 12, the maximum value of the displacement is 0.3237 mm. The simulation also shows that the minimum safety factor is 3.85 that is greater than 2.73 - the allowed safety factor. These results manifest the loading capacity of the designed end-effector with respect to its material and geometry designed.

5. CONCLUSIONS

In this paper, the design of the serial-parallel robotic system handling billet for a given hot forging extrusion station was analyzed in terms of kinematic and strength aspects. The kinematic modeling and analysis clarify the advantage of the kinematic chain designed. By considering the parallel links, the kinematical constraint equation is written and put together with the kinematic model which shows the reduction of the number of joint variables and restriction of the orientation of the end-effector as desired. These features thus reduce the complexity of the robot control program; the robot grips and releases a billet in an efficient and simple manner. The inverse kinematic analysis shows that the manipulator needs only 15s to transfer a hot billet from the heating furnace to the forging die, provided that the velocity of the end-effector is $0.15m/s$. The workspace and the dexterity analysis depicts that, for the given task of transferring billets between the required positions (see Fig. 1), the manipulator is capable of working flexibly. In the active range of joint variables, the manipulability index analysis reveals that no kinematical singularity arises when the robot operates. Besides, the dexterity analysis could be useful for

selecting the proper ratio of the length of links 3 and 4. Finally, by using the finite element method integrated in CAE software, the static stress and displacement distributed on the end-effector are analyzed. The maximum value of the stress and the static deflection of the end-effector computed assess the strength, the safety factor and the loading capability for the robot.

REFERENCES

1. Ceccarelli M., Ottaviano R. - Kinematic design of manipulator, InTech Publisher (2008).
2. Wang J., Li Y., Zhao X. - Inverse kinematics and control of a 7dof redundant manipulator based on the closed loop algorithm, International Journal of Advanced Robotic Systems **7** (4) (2010) 1-9.
3. Li Y., Xu Q. - Kinematic analysis of a 3-PRS parallel manipulator, Robotics and Computer Integrated Manufacturing **23** (2007) 395-408.
4. Merlet J. P. - Parallel robots, London Kluwer Academic Publishers (2000).
5. Razali Z. B., Yatim N. - Conceptual design of automatic manipulator for metal and non-metal waste management application, International Journal of Emerging Technology and Advanced Engineering **3** (2013)10-14.
6. My C. A. et al. - Mechanical design and dynamics modelling of ropc robot, Proceedings of IFToMM International Symposium on Robotics and Mechatronics, Hanoi, Vietnam (2009) 92-96.
7. Sakai S., Iida M., Osuka K., Umeda M. - Design and control of a heavy material handling manipulator for agricultural robots, Auton Robot **25** (2008) 189-204.
8. Maeda S., Tsujiuchi N., Koizumi T., Sugiura M., Kojima H. - Development and control of a pneumatic robot arm for industrial fields, Int. J. Adv. Robotic Sy. **9** (2012)59-66.
9. Song J., Mou J. I., King C. - Parallel kinematic machine positioning accuracy assessment and improvement, Journal of Manufacturing Processes **2**(1) (2000) 48–58.
10. Dwivedy S. K., Eberhard P. - Dynamic analysis of flexible manipulators, a literature review, Mechanism and Machine Theory **41** (2006) 749-777.
11. Prabhu N., Anand M. D., Ruban L. E. - Structural analysis of Scorbot-ER Vu plus industrial robot manipulator, Production & Manufacturing Research: An Open Access Journal **2** (1) (2014) 309-325.
12. Sypkens S. M., Bronsvoort W. F. - Integration of design and analysis models, Journal of Computer-Aided Design & Applications **6** (2009) 795–808.